

# Effects of Buffer Thickness on ATW Blanket Performance

W. S. Yang

*Chosun University*  
375 Seosuk-dong, Dong-gu, Kwangju, 501-759, Korea  
wsyang@chosun.ac.kr

and

L. Mercatali, T. A. Taiwo, R. N. Hill

*Argonne National Laboratory*  
9700 South Cass Avenue, Argonne, Illinois 60439  
mercatali@anl.gov; Taiwo@anl.gov; BobHill@anl.gov

**Abstract** - *This paper presents preliminary results of target and buffer design studies for liquid metal cooled accelerator transmutation of waste (ATW) systems, aimed at maximizing the source importance while simultaneously reducing the irradiation damage to fuel. Using 840 MWt liquid metal cooled ATW designs, the effects of buffer thickness on the blanket performance have been studied. Varying the buffer thickness for a given blanket configuration, system performance parameters have been estimated by a series of calculations using the MCNPX and REBUS-3 codes. The effects of source importance variation are studied by investigating the low-energy (< 20 MeV) neutron source distribution and the equilibrium cycle blanket performance parameters such as fuel inventory, discharge burnup, burnup reactivity loss, and peak fast fluence. For investigating irradiation damage to fuel, the displacements per atom (dpa), hydrogen production, and helium production rates are evaluated at the buffer and blanket interface where the peak fast fluence occurs. Results for the liquid-metal-cooled designs show that the damage rates and the source importance increase monotonically as the buffer thickness decreases. Based on a compromise between the competing objectives of increasing the source importance and reducing the damage rates, a buffer thickness of around 20 cm appears to be reasonable. Investigation of the impact of the proton beam energy on the target and buffer design shows that for a given blanket power level, a lower beam energy (0.6 GeV versus 1 GeV) results in a higher irradiation damage to the beam window. This trend occurs because of the increase in the beam intensity required to maintain the power level.*

## I. INTRODUCTION

The accelerator-driven systems (ADSs) have been considered in several countries for treating spent fuel and generating power.<sup>1</sup> In these systems, a high-power particle accelerator produces energetic protons that interact with a heavy metal target to produce neutrons. The source neutrons are generated by direct impingement of the accelerator proton beam onto a target material in a process called spallation. The spallation neutrons are subsequently multiplied in the surrounding subcritical blanket. The spallation target and the subcritical blanket are coupled through a buffer region, which helps the spallation neutrons

to diffuse into the blanket and reduces the damage to fuel by high-energy neutrons.

The target and buffer designs should be performed in conjunction with the blanket design. The source-driven multiplication factor of a given blanket design increases as the source importance increases. Thus, by designing target and buffer for a higher source importance,<sup>2</sup> the desired multiplication factor at the beginning of cycle (which is determined by a compromise between the competing objectives of minimizing accelerator power and precluding the potential for criticality) can be achieved with a reduced amount of fuel. The reduced fuel loading would increase the discharge burnup for a fixed fuel residence time. This

indicates that the target position and the buffer thickness need to be determined such that the source importance is maximized. At the same time, the peak damage to fuel needs to be reduced to increase the fuel residence time and hence the discharge burnup. Therefore, the target position and buffer thickness need to be optimized based on a compromise between these competing objectives.

The effects of buffer thickness on the blanket performances were studied for two 840-MWt ATW designs using lead-bismuth-eutectic (LBE) and sodium as coolant. Varying the buffer thickness for a given blanket configuration, system performances were estimated by a series of calculations using MCNPX and REBUS-3 codes.<sup>4,5</sup> The effects of source importance change were studied by investigating the low-energy (< 20 MeV) neutron source distribution and the equilibrium cycle blanket performance parameters such as fuel inventory, discharge burnup, burnup reactivity loss, and peak fast fluence. For investigating the irradiation damage to fuel, the dpa, hydrogen production, and helium production rates were evaluated at the buffer and blanket interface where the peak fast fluence occurs.

The results of these parametric studies are summarized in this paper. Computational model and methods are first described in Section II. The results of parametric studies are discussed in Section III. Specifically, the low-energy neutron source distribution, the equilibrium-cycle blanket performance parameters, and the damage rates are compared. Section IV contains the conclusions from the current studies and a discussion of future activities.

## II. COMPUTATIONAL MODEL AND METHODS

The effects of buffer thickness on the blanket performances were studied using the 840 MWt liquid-metal-cooled ATW designs described in Ref. 3. These designs were developed to achieve the main objective of high discharge burnup while meeting key thermal-hydraulic and materials-related design constraints. The blanket was assumed to be fueled with a non-uranium metallic dispersion fuel; pyrochemical techniques are used for recycle of residual transuranic actinides (TRU) in this fuel after irradiation. Fig. 1 displays an R-Z model of the LBE-cooled ATW design used in this study; the blanket region was divided into 3 enrichment zones, 25 depletion regions. In this reference configuration, the LBE target region is 169.6 cm high and 8.5 cm in radius, and is surrounded by a 28.6 cm thick LBE buffer. The R-Z model for the sodium-cooled ATW design is quite similar, with the exception that this design has a more compact blanket (67.6 cm thickness versus 98.5 cm for the LBE-cooled design). The compactness of the sodium-cooled ATW design derives from the fact that the corrosion control approach that is employed in the LBE-cooled design, and which limits the coolant velocity, is not used in the sodium-cooled design.<sup>3</sup>

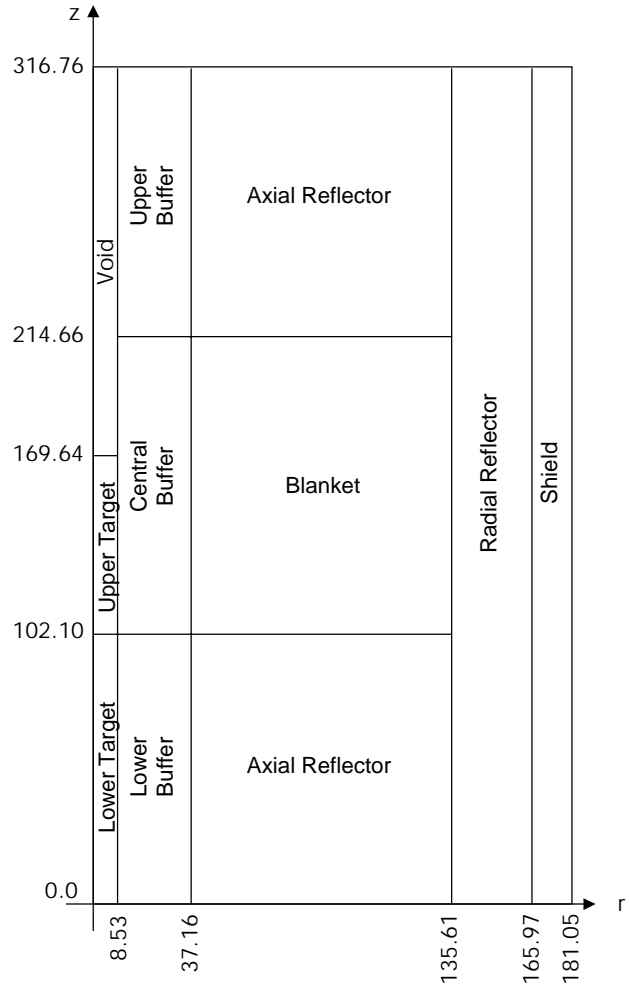


Fig. 1. R-Z Model of 840 MWt LBE Cooled ATW System Design (Base Case).

Because the sodium-cooled design can exploit a higher coolant velocity, the fuel volume fraction can be higher and a more compact design is achieved. Additionally, the compact sodium-cooled blanket requires only two enrichment zones to achieve acceptable power peaking factors. The geometric dimensions of the target and buffer zones and the target material (LBE) are the same for the two designs.

The buffer thickness was varied from the reference value of 28.6 cm to 11.5 cm, while the blanket volume was kept constant. For a 1 GeV proton beam impinging on the top surface of the LBE target with a uniform radial distribution, system performances were estimated by a series of calculations using MCNPX and REBUS-3 codes. A modified version of MCNPX was used in this study. In this modified version of MCNPX, each neutron is killed if its energy is below a cutoff energy, and its weight, location, direction, and energy are stored on a log file. A low-energy

neutron source distribution for a given transmuter configuration can be obtained by processing this log file.

For each buffer configuration, the spallation neutron source distribution was first determined from an MCNPX calculation by setting the neutron cutoff energy to 20 MeV. The beginning of equilibrium cycle (BOEC) compositions obtained from a homogeneous eigenvalue calculation of REBUS-3 was used in this source calculation. By performing a fixed-source REBUS-3 calculation using this low-energy source distribution, blanket performances were evaluated for the equilibrium fuel cycle. Assuming a fuel residence time of four years at 75% capacity factor with a cycle length of one half year, the TRU-10Zr particle fraction in fuel was determined such that the source-driven multiplication factor at BOEC is 0.97. In the reference designs, the fuel residence time of the innermost fuel assemblies are less than that for the others in order to satisfy the peak fast fluence limit of  $4.0 \times 10^{23}$  n/cm<sup>2</sup>. However, this constraint was not imposed in this study, and the fuel residence time was eight cycles for all assemblies. The fuel was depleted at a constant power level by increasing the source intensity over an irradiation cycle to compensate the burnup reactivity loss. The blanket compositions at BOEC and the end of equilibrium cycle (EOEC) were determined from this calculation. Finally, the damage rates of structural

material were estimated for the BOEC and EOEC configurations by performing MCNPX calculations with the neutron cutoff energy of zero.

### III. RESULTS AND DISCUSSIONS

#### III.A. Impact of Buffer Thickness on System Performance

The effects of buffer thickness on the low-energy (< 20 MeV) neutron source distribution and the equilibrium cycle blanket performance for the LBE-cooled design are summarized in Table I. The low-energy source distributions were generated using 100,000 protons, and the estimated standard deviations for the neutron production per proton were ~0.3%. The source importance factor<sup>2</sup> shown in Table I represents the probability for an external neutron to cause a fission reaction relative to a fission neutron. It was estimated by the ratio  $(1/k_{\text{eff}} - 1)/(1/k_s - 1)$ , where  $k_s$  is the source-driven multiplication factor determined using the actual flux distribution of the source-driven problem and  $k_{\text{eff}}$  is the effective multiplication factor obtained from the corresponding eigenvalue calculation.

The number of low-energy source neutrons produced per proton is relatively insensitive to the buffer thickness (see Table I). The spatial distribution is also insensitive to

TABLE I

Low-Energy Source Distribution and Equilibrium Cycle Blanket Performances for LBE-Cooled ATW Design

Case	Base	1	2	3	4
Buffer thickness (cm)	28.6	26.8	23.9	18.4	11.5
Relative volume	1.00	0.90	0.75	0.50	0.25
Low-energy neutron source per proton	28.96	28.93	28.85	28.72	28.41
Source neutron distribution (%)					
Upper target	55.30	55.37	55.54	55.83	56.34
Lower target	0.33	0.33	0.32	0.33	0.34
Upper buffer	0.16	0.15	0.14	0.11	0.08
Central buffer	32.90	32.20	30.87	27.78	22.18
Lower buffer	2.62	2.50	2.25	1.73	1.04
Blanket	6.60	7.23	8.43	11.32	16.49
Others	2.09	2.22	2.45	3.40	3.53
Equilibrium cycle performances					
BOEC TRU inventory (kg)	3085	3074	3048	3004	2961
Burnup reactivity loss (%)	5.30	5.24	5.16	5.02	4.87
Discharge burnup (atom %)	28.2	28.3	28.5	28.8	29.2
Peak fast fluence ( $\times 10^{23}$ n/cm <sup>2</sup> )	4.31	4.44	4.74	5.44	6.64
Power peaking factor					
BOEC	1.358	1.361	1.370	1.386	1.402
EOEC	1.488	1.517	1.584	1.741	2.024
Source importance factor					
BOEC	0.801	0.817	0.843	0.891	0.952
EOEC	0.788	0.803	0.827	0.871	0.926

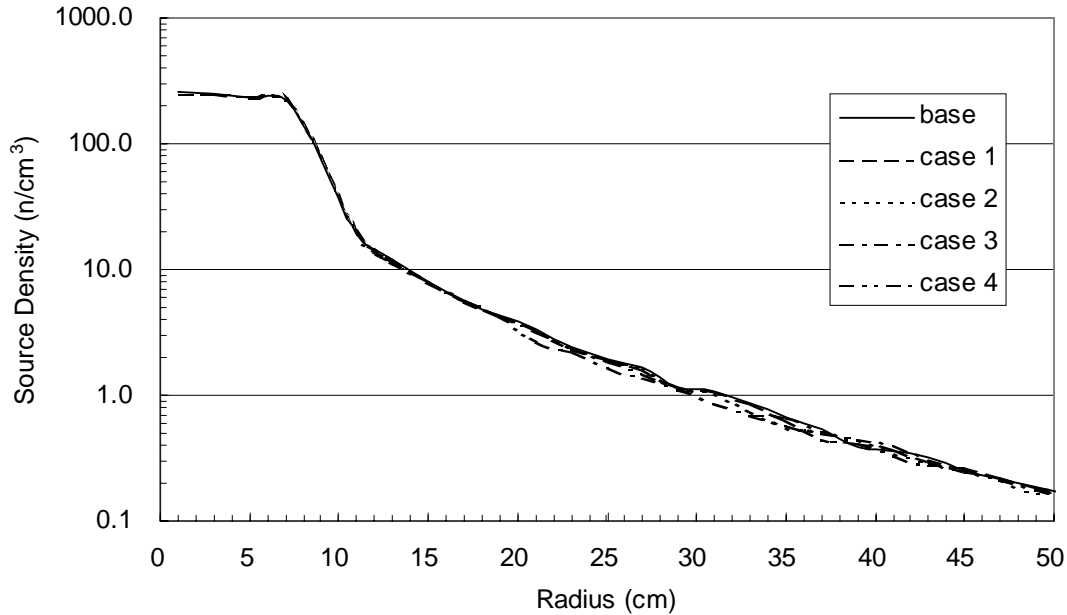


Fig. 2. Radial Distributions of Low-Energy Neutron Sources at Blanket Midplane for LBE-Cooled ATW Design.

the buffer thickness. As shown in Fig. 2, the radial distributions of low-energy neutron sources at the blanket midplane are practically independent of the buffer thickness. It was also found that the axial distributions at a fixed radius are practically independent of the buffer thickness. These results show that the low-energy neutron source distribution does not depend on the buffer thickness strongly in the range of the buffer thickness considered in this study. However, the number of source neutrons produced in each region strongly depends on the buffer thickness. Among about 29 low-energy source neutrons produced per proton, ~55% are produced in the upper target region that has a relatively small volume, and ~39% are produced in the central buffer and blanket regions. As the buffer thickness decreases, the fraction of source neutrons produced in the central buffer decreases, and that in the blanket increases; however, the sum of two fractions remains almost constant. For example, when the buffer thickness is reduced to 11.5 cm from 28.6 cm, the fraction of low-energy source neutrons produced in the blanket increases by a factor of 2.5. This behavior seems to be due to the leakage of high-energy (> 20 MeV) spallation neutrons into the blanket.

To investigate the effects of secondary neutrons in more detail, separate MCNPX calculations were performed using a cylindrical LBE target with a radius of 20 cm and a height of 100 cm and a practically infinite target. The results showed that a 1 GeV proton directly produced 14.8 neutrons of which about 2.4 neutrons were above 20 MeV. These high-energy neutrons produced 8.8 high-energy neutrons

and about 0.7 low-energy neutrons additionally. Among 8.8 high-energy neutrons, about 1.4 neutrons leaked out from the region of 20 cm radius and 100 cm height, and the other neutrons were slowed down below 20 MeV. The neutrons leaking out of the inner region produced 7.8 additional source neutrons in the outer region. These results indicate that high-energy neutrons produce significantly larger number of low-energy source neutrons by successive nuclear interactions. Thus, as the buffer thickness decreases, more high-energy neutrons leak into the blanket and produce additional source neutrons in the blanket region by nuclear interaction or fission. In addition, since the low-energy source neutrons produced in the blanket have higher probabilities to cause a fission reaction than those produced in the other regions, the source importance increases as the buffer thickness decreases.

The results for the sodium-cooled ATW design are also generally quite similar to those for the LBE-cooled design. A closer examination of the results indicated, however, that the sodium-cooled design yields a slightly lower number of neutrons per incident proton, and also shows a stronger variation in this quantity as the buffer thickness is varied. This trend is due to the fact that sodium has a lower atomic number than LBE, and hence the latter has better spallation-neutron production characteristics, similar to those of the target and buffer regions. Because of this, the variation in the number of neutrons produced per incident proton is small for the LBE-cooled design. However, as a result of the smaller neutron-production capability in

sodium-cooled-blanket relative to that of the buffer, moving the blanket region closer (by reducing the buffer thickness) results in a decrease in the number of source neutrons created in the system. The reduction in the total number of neutrons produced per proton in the sodium-cooled design also indicates an increase in the accelerator current requirements. A higher current would result in higher neutron intensity in the target and higher irradiation damage to the beam window.

The results of equilibrium cycle analyses using REBUS-3 show that the system blanket performance generally improves with reduction in the buffer thickness. The BOEC TRU inventory required to achieve a desired source-driven multiplication factor decreases as the buffer thickness decreases. As a result, the average discharge burnup increases, and the burnup reactivity loss decreases with decreasing buffer thickness. When the buffer thickness is reduced to 11.5 cm from 28.6 cm (see Table I), the source importance factor estimated by the diffusion theory increases by ~19%. However, the peak fast fluence and the power peaking factor also increase as the buffer thickness decreases. Especially, the power peaking factor at EOEC increases drastically because of the increased spallation source intensity (to maintain a constant power) and non-uniform TRU depletion. (The peak power density at BOEC occurs in the middle fuel zone due to the enrichment splitting employed to flatten the power distribution, but it moves to the innermost fuel zone at EOEC because of the

increased source intensity.)

As discussed in previous studies,<sup>6,7</sup> the maximum discharge burnup achievable under various key design constraints is mainly determined by the peak fast fluence limit. Thus, it is desirable to minimize the peak fast fluence per unit discharge burnup. At the same time, the burnup reactivity loss needs to be minimized to reduce the accelerator power or other control requirement. Therefore, for a more consistent comparison, the reactivity loss per unit discharge burnup and the peak fast fluence per unit discharge burnup are compared. As shown in Fig. 3, the reactivity loss per unit discharge burnup decreases monotonically as the buffer thickness decreases. On the other hand, the peak fast fluence per unit discharge burnup increases monotonically. While the burnup reactivity loss per unit discharge burnup decreases almost linearly, the peak fast fluence per unit discharge burnup increases more steeply as the buffer thickness decreases. Based on a compromise between the competing objectives of minimizing the burnup reactivity loss and the peak fast fluence, a buffer thickness of ~20 cm appears to be reasonable.

### III.B. Damage Rates at the Buffer and Blanket Interface

In addition to the evaluation of system performance with target and buffer design, the impact of the design on the damage rates has also been investigated. Table II summarizes the effects of buffer thickness on the damage

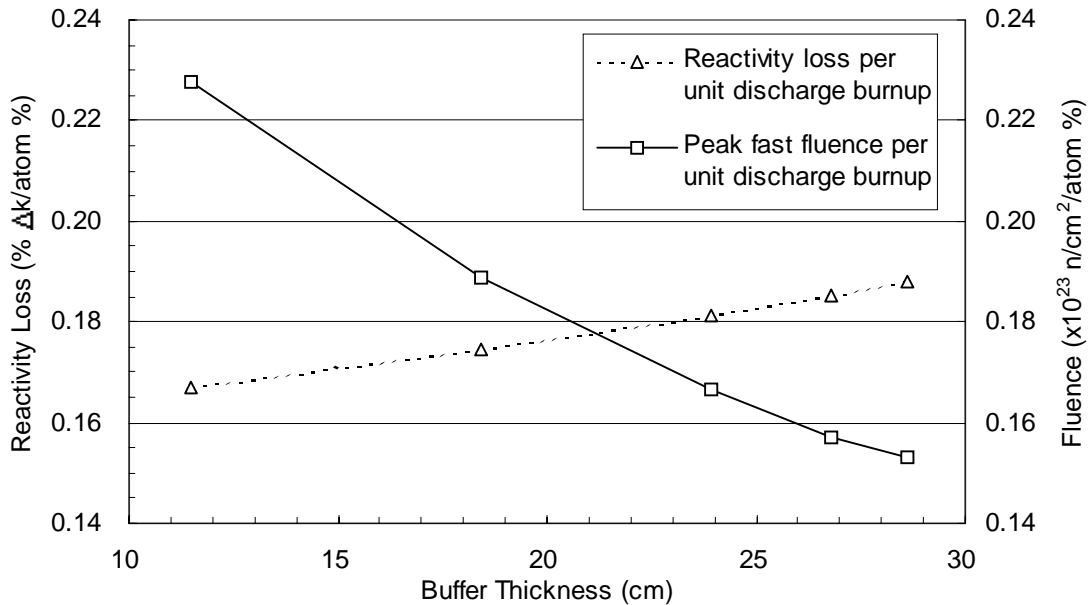


Fig. 3. Burnup Reactivity Loss and Peak Fast Fluence per Unit Discharge Burnup (LBE-Cooled Design).

rates of structural material at the buffer and blanket interface for the LBE-cooled design. These damage rates (dpa, hydrogen production, and helium production) were determined by renormalizing the results obtained from MCNPX calculations to the power level of 840 MWt. The MCNPX calculations were performed with 1,000 protons in order to limit each computational time to a reasonable amount (~20 hours). The resulting standard deviations of neutron induced damage rates were ~5%, but proton induced ones were typically around 50%. (The standard deviations of

proton induced damage rates of case 2 were close to 100%.) The proton-induced dpa rates were negligible (less than 0.1%) compared to the neutron induced one, and hence they are not included in Table II. The low-energy neutron induced hydrogen and helium production rates were evaluated for HT-9, but the others were evaluated for iron.

The dpa in iron is mainly induced by low-energy (< 20MeV) neutrons, as shown in Table II. However, for the hydrogen and helium production, the high-energy neutron contributions are larger than the others. Especially, the

TABLE II

Peak Damage Rates of Structural Material at Buffer and Blanket Interface (LBE-cooled ATW Design)

Case	Base	1	2	3	4
Peak dpa rate of Iron (dpa/year)					
BOEC Low-energy neutron	42.09	45.90	46.35	51.42	59.50
High-energy neutron	0.21	0.24	0.29	0.49	1.25
Sum	42.30	46.14	46.64	51.91	60.75
EOEC Low-energy neutron	61.36	62.63	68.45	80.77	100.77
High-energy neutron	0.41	0.41	0.59	1.11	2.37
Sum	61.77	63.04	69.04	81.88	103.14
Average Low-energy neutron	51.72	54.27	57.40	66.10	80.14
High-energy neutron	0.31	0.32	0.44	0.80	1.81
Sum	52.03	54.59	57.84	66.90	81.94
Peak H production rate (appm/year)					
BOEC Low-energy neutron (HT9)	35.33	36.29	38.93	53.55	84.86
High-energy neutron (Fe)	60.58	73.22	112.93	174.17	346.70
Proton (Fe)	3.88	2.06	5.09	12.32	48.33
Sum	99.79	111.56	156.94	240.04	479.88
EOEC Low-energy neutron (HT9)	57.32	61.45	73.68	107.25	204.07
High-energy neutron (Fe)	128.49	150.48	200.54	377.03	742.90
Proton (Fe)	4.40	4.10	7.16	31.43	229.40
Sum	190.21	216.02	281.38	515.71	1176.38
Average Low-energy neutron (HT9)	46.33	48.87	56.31	80.40	144.47
High-energy neutron (Fe)	94.54	111.85	156.73	275.60	544.80
Proton (Fe)	4.14	3.08	6.12	21.87	138.87
Sum	145.00	163.79	219.16	377.87	828.13
Peak He production rate (appm/year)					
BOEC Low-energy neutron (HT9)	3.48	3.09	3.82	6.95	11.34
High-energy neutron (Fe)	3.04	3.66	5.66	8.66	17.55
Proton (Fe)	0.11	0.07	0.17	0.44	1.75
Sum	6.63	6.82	9.64	16.05	30.64
EOEC Low-energy neutron (HT9)	6.93	6.69	8.60	14.16	31.34
High-energy neutron (Fe)	6.39	7.44	10.09	19.17	38.11
Proton (Fe)	0.11	0.15	0.27	1.03	8.41
Sum	13.42	14.28	18.96	34.35	77.86
Average Low-energy neutron (HT9)	5.20	4.89	6.21	10.55	21.34
High-energy neutron (Fe)	4.71	5.55	7.87	13.92	27.83
Proton (Fe)	0.11	0.11	0.22	0.73	5.08
Sum	10.02	10.55	14.30	25.20	54.25

high-energy neutron induced hydrogen production rates are several times larger than the low-energy neutron induced ones. The damage rates increase monotonically as the buffer thickness decreases, since the buffer and blanket interface moves toward a higher flux zone. The damage rates of case 1 are lower than those of the base case for the hydrogen production rates induced by proton and the helium production rates induced by low-energy neutron and proton, but they are believed to be due to the fluctuation of the source-driven multiplication factor used in the normalization process. In REBUS-3 calculations for determining the fuel particle fraction in the dispersion fuel, the convergence criterion for source-driven multiplication factor was 0.001. However, the source-driven multiplication factor estimated from MCNPX calculations showed a larger fluctuation. The source-driven multiplication factors of the case 1 were larger than those of the base case by 0.3% and 0.4% at BOEC and EOEC, respectively. As a result, the proton beam current required for a constant power was lower for the case 1 than for the base case. Consequently, the damage rates of case 1 were relatively underestimated.

As shown in Fig. 2, the source density increases exponentially as the distance from the target decreases. Therefore, as the buffer thickness decreases, the innermost fuel zone experiences a much higher flux level and hence a much higher irradiation damage. Furthermore, since the source neutron spectrum is harder than the fission neutron spectrum, the damage rates induced by high-energy neutrons are more severe at reduced buffer thickness. This can be

observed from the high-energy damage rates shown in Table II; the damage rates induced by high-energy neutrons and protons increase much more rapidly as the buffer thickness decreases than those induced by low-energy neutrons.

By comparing the peak fast fluence in Table I and the dpa rates of iron in Table II, it can be observed that the dpa is proportional to the fast fluence. These results show that one dpa corresponds to  $2.7 \times 10^{21}$  n/cm<sup>2</sup> (above 0.1 MeV). This is somewhat larger than the value of  $\sim 2 \times 10^{21}$  n/cm<sup>2</sup> observed in EBR-II for 20% cold worked 316 stainless steel cladding.<sup>8</sup> However, these results indicate that the dpa can be related to the fast fluence and hence can be estimated using the fast fluence that is easier to calculate.

As discussed above, the peak power density location moves to the innermost fuel zone, and hence the damage rates at the buffer and blanket interface increase over an irradiation cycle. Furthermore, the power peaking factor also increases as the buffer thickness decreases. Especially, the power peaking factor at EOEC increases drastically because of the increased spallation source intensity and non-uniform TRU depletion. As a result, the damage rates at EOEC increase more rapidly as the buffer thickness decreases than the BOEC damage rates. The cycle-averaged total damage rates increase more steeply with decreasing buffer thickness as shown in Fig. 4. In particular, the hydrogen production rate increases very rapidly when the buffer thickness becomes thinner than  $\sim 18$  cm.

The trends in the damage rates for the sodium-cooled design are generally quite similar as those presented above

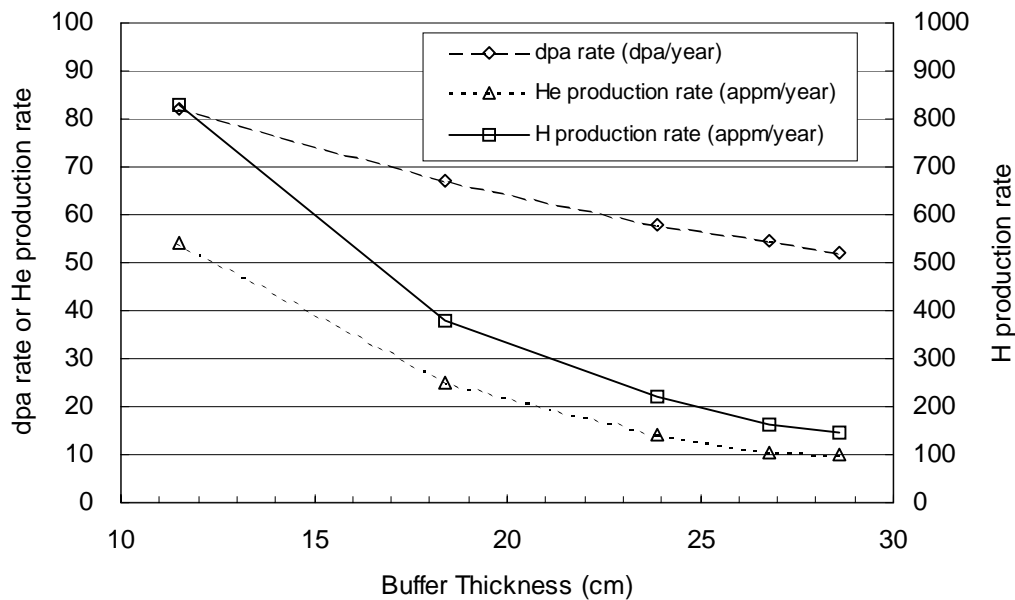


Fig. 4. Cycle-Averaged Damage Rates vs. Buffer Thickness for the LBE-Cooled ATW Design.

for the LBE-cooled design. However, we note as aforementioned that the irradiation damage at the beam window is expected to be higher in the sodium-cooled design because of the higher beam intensity required to offset the lower number of source neutrons produced, relative to the LBE-cooled design. Additionally, we found that the dpa rate at the buffer and blanket interface is slightly lower in the LBE-cooled design, because the neutron spectrum in the energy region from ~1 to 20 MeV is lower for the LBE-cooled design. The gas production rates, which are dominated primarily by the high-energy component, were found to be higher in the sodium-cooled design.

### III.C. Impact of Incident Proton Beam Energy on Damage Rates

An investigation of the impact of incident proton beam energy on the damage rates has been performed for a sodium-cooled ATW design with a buffer thickness of 20 cm. Calculations were done using MCNPX for incident proton energies of 0.6 and 1 GeV. In these calculations, 10,000 protons were used to start the stochastic coupled-particle simulation for the whole energy range (0 to 1 GeV). Results of this study are summarized in Table III. The results show that a reduction of the beam energy from 1 GeV to 600 MeV leads to an increase in the damage rates at the window and has only small impact on the rates at the

buffer and blanket interface.

For the same blanket power, the beam intensity of the 600 MeV case needs to be increased by a factor of 2.1 to offset the lower number of neutrons produced per incident proton. As a result, the proton-induced hydrogen and helium production rates at the window are increased by a factor of 1.9 and 1.8, respectively. (The increase of the gas production rates is slightly lower than that of the proton intensity since the damage rates per proton decrease with decreasing particle energy.) The total number of source neutrons is increased by ~3% because of the relatively lower energy of product neutrons. The neutron-induced damage rates at the window are increased by 10~20% because of the higher density and harder spectrum of source neutrons near the window.

At the interface, the variations of damage rates show somewhat complicated behaviors. Despite the higher proton beam intensity, the number of protons reaching the interface is lower for the 600 MeV case, since the range of proton decreases with decreasing energy. As a result, the proton-induced hydrogen and helium production rates are reduced by ~72% and ~78%, respectively. The damage rates induced by low-energy neutrons are increased slightly due to the higher source intensity. (Relative to the window, the impact of the higher source intensity is reduced at the interface because the fission neutrons dominate in the low-energy neutron population.) However, the damage rates

TABLE III  
Effects of Beam Energy on the Peak Damage Rates of the Sodium-Cooled ATW

Parameter	Beam energy			
	1 Gev		600 Mev	
Proton Current intensity, mA	13.34		28.19	
Proton Current density, $\mu\text{A}/\text{cm}^2$	58.47		123.55	
Neutron per incident proton, n/p	26.72		13.05	
Peak Damage Rate	Window	Interface	Window	Interface
dpa rate of Iron (dpa/year)				
Low energy neutron	114.92	81.98	132.34	83.95
High energy neutron	6.51	1.37	7.69	1.52
Sum	121.43	83.35	140.03	85.47
H production rate (appm/year)				
Low energy neutron (HT-9)	836.92	179.49	975.35	189.15
High energy neutron (Fe)	1579.02	405.92	1739.10	391.24
Proton (Fe)	287.17	28.13	556.04	7.79
Sum	2703.11	613.54	3270.49	588.18
He production rate (appm/year)				
Low energy neutron (HT-9)	185.15	28.68	213.50	33.44
High energy neutron (Fe)	77.12	20.82	85.13	19.41
Proton (Fe)	6.44	0.94	11.62	0.21
Sum	268.71	50.44	310.25	53.06

induced by high-energy neutrons are determined by the relative magnitude of two opposite effects of the increased intensity and the reduced energy of source neutrons; the dpa rate is increased slightly, but the gas production rates are decreased slightly. The overall damage rates are determined by the relative magnitude of individual components; the dpa and helium production rates are slightly higher for the case using the 600 MeV beam, but the hydrogen production rate is slightly lower.

Simulations were also performed to investigate the contributions to the damage induced by fission and spallation neutrons separately. For this purpose a calculation without the subcritical medium and with a 1 GeV beam was done. The results of this investigation show that the interface is more sensitive to the presence of the blanket than the window, in terms of radiation damage, as would be expected. Neutrons generated in the multiplier region have a high probability to reach the interface between the buffer and blanket and a small amount of those are likely able to diffuse through the buffer and to add a component to the neutron spectrum in the window. The low energy dpa rate is higher by a factor of ~8 in the interface and ~1.9 in the window when the blanket is present. Simulations also show relatively higher low-energy hydrogen and helium gas production rates in the interface for the case with blanket (~84% and ~16% for hydrogen and helium, respectively).

#### IV. CONCLUSIONS

Target and buffer design studies have been done to investigate the impact of buffer thickness on transmuter performance and irradiation damage for LBE-cooled and sodium-cooled ATW designs. The results for the two designs have also been intercompared. The primary difference between the two designs is that the number of neutrons produced per proton for the sodium-cooled design varies more significantly with reduction in the buffer thickness, while that in the LBE-cooled design is fairly constant. Generally, however, the trends in system performance and irradiation damage rates are similar for the two designs, as the buffer thickness is varied. In particular, the source importance increases significantly (by as much 20%) as the buffer thickness is reduced from 28.6 to 11.5 cm. The burnup reactivity loss was found to decrease (~10%) with reduction in buffer thickness. However, the reduced buffer thickness results in large (~50%) increases in the fluence/burnup ratio, implying a much lower discharge burnup for a given fluence limit. In addition, the high-energy damages are much more severe at reduced buffer thickness. Thus, a clear design trade-off between increased accelerator size/cost (thick buffer) and increased fuel processing demand (reduced burnup with thin buffer) is emerging.

Additional studies were also performed to investigate the impact of the incident proton beam energy on the

target-buffer design. The primary finding from this case is that the damage rates at the beam window is increased as the beam energy decreases, because the beam strength has to increase to attain the same power level in the blanket, as the higher energy case.

Based on the compromise between the competing objectives of increasing the source importance and reducing the irradiation damage, a buffer thickness of ~20 cm appears to be reasonable. However, in order to make more definite conclusions, further studies need to be performed. In particular, it is necessary to investigate the combined effects of various irradiation damage components and to devise the design criteria for the irradiation damage of structural materials using actual irradiation data.

#### REFERENCES

1. A Roadmap for developing Accelerator Transmutation of Waste (ATW) Technology; A Report to Congress, DOE/RW-0519, US Dept. of Energy, Oct. 1999.
2. M. SALVATORES, I. SLESSAREV, A. TCHISTIAKOV, and G. RITTER, "The Potential of Accelerator-Driven Systems for Transmutation or Power Production Using Thorium or Uranium Fuel Cycles," *Nucl. Sci. Eng.*, **126**, 333 (1997).
3. W. S. YANG, T. A. TAIWO, R. N. HILL, H. S. KHALIL, D. C. WADE, "Performance Comparison of Liquid Metal and Gas-Cooled ATW System Point Designs," *ICONE-9; Ninth International Conference on Nuclear Engineering*, Nice, France, April 8-12, 2001.
4. H. HENRYSON II, B. J. TOPPEL, and C. G. STENBERG, "MC<sup>2</sup>-2: A Code to Calculate Fast Neutron Spectra and Multigroup Cross Sections," ANL-8144, Argonne National Laboratory (1976).
5. L. S. WALTERS, "MCNPX Users Manual (Version 2.1.5)," APT Program Report, Los Alamos National Laboratory, November 14, 1999.
6. W. YANG and H. KHALIL, "Blanket Design Studies of an LBE Cooled Accelerator Transmutation of Waste System," *Nuclear Technology* (to be published).
7. W. S. YANG, D. G. NABEREJNEV, and H. S. KHALIL, "Physics Design Optimization of an LBE Cooled ATW Blanket," *Trans. Am. Nucl. Soc.*, **83**, 328 (2000).
8. A. E. WALTER and A. B. REYNOLDS, *Fast Breeder Reactors*, Pergamon Press, Elmsford, New York, U.S.A., (1981).